Electrostatic Probe Measurements in Solid-Propellant Rocket Exhausts

GEORGE MAISE* AND ALBERTO J. SABADELL†
AeroChem Research Laboratories, Inc., a subsidiary of Sybron Corporation, Princeton, N.J.

A stagnation point electrostatic probe that can be used to measure local electrical characteristics of solid-propellant rocket exhausts has been developed. The probe is a flat-faced insulated cylinder with the collector surface at the tip, and is water-cooled. The probe was tested in a laboratory flame and in small-scale rocket motor exhausts at the Naval Research Laboratory, and performed well both thermally and electrically. The analytical procedure for interpreting probe measurements was based on Lam's generalized continuum theory. The theory was verified in laboratory flames of known ionization levels. Positive ion and electron densities were measured in small-scale aluminized composite solid-propellant rocket motor exhausts at NRL. Tests in full-scale, sea-level rocket motor exhausts were performed, and positive ion densities in general agreement with theoretical predictions were obtained. It is concluded that local values of charged species concentrations in solid-propellant rocket motor exhausts can be obtained with a stagnation point electrostatic probe.

Nomenclature

D = diffusion coefficient
e = electron charge
f = velocity function
I = charged species concentration gradient defined by Eq. (18)
$\bar{I}$ = charged species concentration gradient defined by Eq. (16)
J = current density
l = plume nutation travel distance
L = probe radius
n = charged species number density
N = normalized number density, $n/n_{e\infty}$
P = potential
R = electric Reynolds number, $\epsilon U_\infty L/D_i$
Re = Reynolds number
$\bar{s}$ = Lees-Dorodnitsyn coordinate defined by Eq. (10)
T = temperature
u = velocity directed along x axis
U_∞ = velocity in the undisturbed plasma
v = velocity directed along y axis
x = distance parallel to probe surface, Fig. 3
y = distance normal to probe surface, Fig. 3
y_{sh} = thickness of electrostatic sheath
$\alpha'_1(0)$ = charged species concentration gradient, Table 2
β = $D_i/\epsilon D_e$
$\bar{\beta}$ = velocity gradient at the edge of boundary layer, $\partial u_e/\partial x$
δ = boundary-layer thickness
ϵ = T_i/T_e
η = nondimensionalized coordinate defined by $yR^{1/2}/L$
$\bar{\eta}$ = Lees-Dorodnitsyn coordinate defined by Eq. (11)
η^* = distance to edge of sheath
λ = mean free path
μ = viscosity
ρ = density

Subscripts

e = electrons, also edge of boundary layer
B = probe surface
i = ions
n = neutral particle
∞ = freestream
$+$ = positive ions
$-$ = negative ions

Introduction

THE work discussed in this paper was motivated by the need to measure local electron densities in rocket exhaust plumes. Free electrons in the exhaust can attenuate and scatter radar signals. To compute the extent of this interference, one must know the distribution of electrons along the path of the radar beam. Theoretical models have been developed[1,2] to predict the detailed distribution of electrons in a plume; however, these models have not been verified by direct local measurements. The electrostatic probe is a suitable instrument for measuring local electron and ion densities. The goal of our work was to develop an electrostatic probe system that can be used in rocket test facilities to measure the electrical characteristics of exhaust plumes. This included the development of probe hardware and an analytical procedure to interpret the probe readings (current vs voltage) in terms of electron and ion densities.

Although electrostatic probes have been used for many years to measure the electrical characteristics of plasmas, their use in rocket exhausts has been very limited. A previous research program[3] reported some success on the use of electrostatic probes in liquid-propellant exhausts.

The use of probes in rocket exhausts, particularly solid-propellant exhausts, presents difficulties. The probe is exposed to high temperature, high heat flux, corrosive gases, and erosion by high-speed solid particles (e.g., from aluminized propellants). To maintain the probe at a sufficiently low temperature to prevent electron emission from the surface, internal cooling has to be provided. Theoretically,

Presented as Paper 69-573 at the AIAA 5th Propulsion Joint Specialist Conference, Colorado Springs, Colo., June 9–13, 1969; submitted June 10, 1969; revision received October 31, 1969. This work was supported by the Air Force Rocket Propulsion Laboratory, Edwards, Calif., under Contract FO4611-67-C-0059. R. J. Ronco contributed to the experimental phase of the program. Contributions of H. F. Calcote, D. E. Jensen, S. C. Kurzius, and H. S. Pergament, members of the AeroChem technical staff, are gratefully acknowledged. The small-scale rocket motor tests were conducted at the Naval Research Laboratory in Washington, D.C., in close cooperation with W. W. Balwanz. The sea-level tests were conducted under contract AF 04(611)-11541, also supported by the Air Force Rocket Propulsion Laboratory, Edwards, Calif. The tests were conducted at Thiokol, Huntsville, Ala., in close cooperation with the Thiokol technical staff.

* Aerothermochemist; now associated with Grumman Aircraft Engineering Corp., Bethpage, N.Y. Member AIAA.

† Research Engineer. Member AIAA. All queries concerning this paper should be directed to this author.

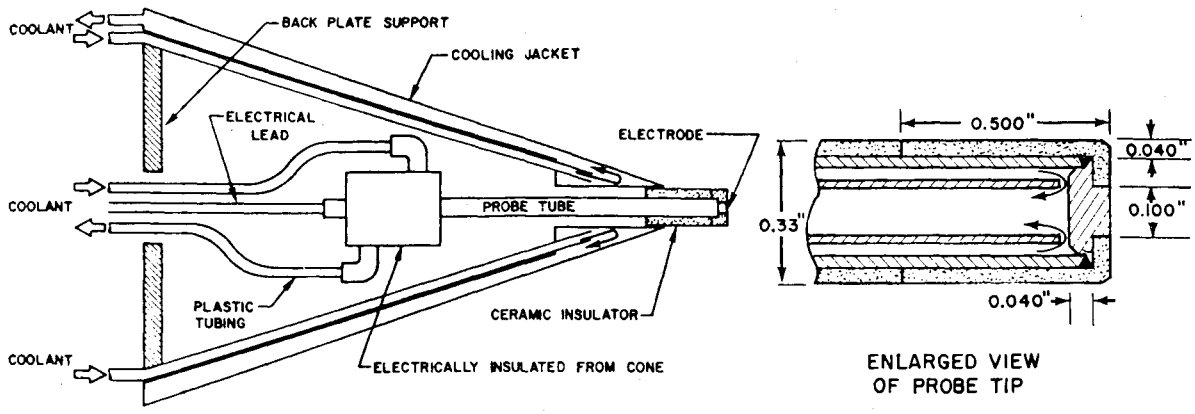

Fig. 1 AeroChem probe AL5.

there are also a number of complications to be overcome. The original no-flow, free-molecular probe theory of Langmuir[4] has been extended by several investigators to take into account collisions in the plasma (e.g., Refs. 5 and 6) and also high-speed flow effects (e.g., Refs. 7 and 8). A rigorous analysis of the heat-transfer effects on a cooled electrode has only recently become available.[9] In addition to the inherent difficulties in the above probe theories, the theoretical interpretation of the probe data in rocket motor exhausts is further complicated by the presence of negatively charged ions and the possibility of shock-induced ionization. All these problems were considered during this program and are discussed in this paper.

Probe Development

Several points must be considered in the design of an electrostatic probe for rocket exhausts. The probe should be as small as possible to minimize distortions of the flowfield and allow for fine spatial resolution. At the same time, it has to be cooled to prevent electron emission and keep the probe tip from melting. The latter requirement indicates that a large probe is desirable. To simplify the theoretical interpretation of the probe readings, the probe should collect ions and electrons only from a small local region of plasma where the fluid mechanical conditions are well defined. The rest of the probe structure must be well insulated from the plasma to prevent spurious leakage currents. A flat-faced cylindrical probe, with the electrode located at the stagnation point was selected for this work. As a compromise, a probe diameter of 0.33 in. was chosen, with the electrode diameter equal to 0.4 times the probe diameter.

Figure 1 shows the design of this probe (AeroChem AL5‡) and the details of the tip construction. The probe consists basically of an internally cooled copper tube closed at one end. The complete probe structure (tube and mounting block) is at the electrode potential; however, everything except a small area (collector surface) at the closed end of the tube is insulated from the plasma. The front part of the tube is insulated by three pieces of ceramic insulation (alumina). The remaining probe structure is coated by a layer of polyvinyl chloride, which is protected thermally from the rocket exhaust by a water-cooled conical shield (stainless steel). The grounded conical shield serves also as the second electrode to complete the electrical circuit.

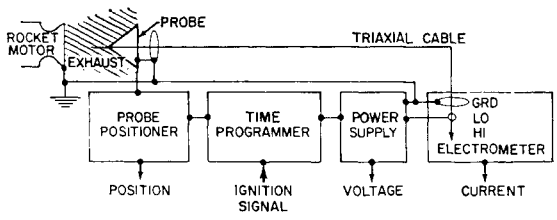

Fig. 2 Probe circuit for rocket motor tests.

‡ Patent pending.

The probe tube (Fig. 1) is closed by a metallic insert which is silver-brazed to the tube. Thus, the high-pressure coolant is contained entirely within a metal structure. The exposed surface of the insert serves as the collecting electrode. An inner tube provides a double passage for the coolant, which, at high pressure, reaches the probe tip through the outer channel. As the coolant passes through the narrow gap between the insert and the inner tube, a strong cooling effect is obtained and the coolant then returns through the inner passage. The metal tube and part of the insert are covered by a ceramic cap. An effective bond between the metal and the ceramic is obtained by first metallizing the inner surface of the ceramic cap and then soft-soldering it to the tube. The two ceramic sleeves behind the cap are mounted in the same way.

The aft ends of the concentric copper tubes are mounted to a brass block to which the inlet and outlet connectors for the coolant are attached. In order to insulate the probe structure effectively from the ground, the coolant is supplied through several feet of high-pressure plastic tubing. Also attached to the block is an electrical lead which supplies the voltage to the probe. The block itself is mounted to a bakelite piece, which, in turn, is attached to the back plate of the cone in such a way that the probe is centered inside the conical shield.

In addition to the electrostatic probe, there are a number of auxiliary items to complete the probe system. The probe is internally cooled by a system that supplies water to the probe at a flow rate of approximately 0.1 lb/sec, at an inlet pressure of 600 psig. To prevent electrical leakage, the water must be either distilled or deionized. The cooling system for the cone differs from that for the probe both in the required quality of the water and in the flow rate. The conical shield can be cooled with tap water. The coolant flow rate is approximately 1.0 lb/sec at 100 psig.

The electrical circuitry to obtain electrostatic probe measurements in rocket motor exhausts is shown in Fig. 2. A triaxial cable connects the probe to the input of a Keithley Electrometer Model 601, which serves as an off-ground current-measuring device. The output of the electrometer (probe current) is recorded on a high-impedance floating recorder. The grounded conical shield of the probe serves as the second electrode. A variable d.c. voltage supply is connected to the probe. The voltage can be varied manually or swept automatically in 0.5 sec; sweeping can be performed continuously for as many cycles as desired.

The over-all operation of the electrostatic probe system is controlled by a multiple circuit time programmer (Multiflex Reset Timer Type HM, Eagle Signal). This is a multiple contact timer provided with a scale for rapid independent

adjustment (Vernier type) of each contact. The time programmer starts operation upon ignition of the rocket motor and the contacts are closed and opened in a preselected sequence. In a typical sequence, the probe first is inserted into the rocket exhaust; an instant later, the preselected voltage sweep is started, and upon completion of the sweep, the probe is retracted from the exhaust.

Theoretical Treatment

The theoretical analysis was directed toward the development of an analytical procedure, to interpret the measured current-voltage characteristic in terms of local electron and ion densities. The approach was to rely as much as possible on existing probe theories and extend them only as required to meet the special conditions of a rocket exhaust. Since we were attempting to measure electron densities under somewhat unusual conditions, complications existed that were neglected in the existing probe theories.

Selection of Probe Theory

A survey of the existing probe theories indicated that Lam's theory[8] might be applicable for the determination of electrical characteristics of rocket exhausts. Lam's theory deals with flowing continuum plasma and requires $\lambda \ll y_{sh} \ll \delta \ll L$. These length scales for a typical sea-level rocket exhaust (Ref. 2, Table 3) and for a probe radius of 0.42 cm are shown in Table 1. (The probe and the various dimensions are also shown schematically in Fig. 3.) Table 1 shows that the required conditions are satisfied and Lam's theory is applicable. The first condition ($\lambda \ll y_{sh}$) need not be satisfied if only saturation conditions are considered. The second condition ($y_{sh} \ll \delta$) can present a limitation at low ionization levels. Since y_{sh} is proportional to $n_e^{-1/3}P^{2/3}$, at low values of n_e and/or high P the sheath can extend beyond the boundary layer and saturation will not occur. The third condition ($\delta \ll L$) requires that the flow velocity be sufficiently high to keep the boundary layer thin. The possible error introduced by failure to meet this requirement is on the order of $Re^{-1/2}$. The theory has some additional limitations, which are discussed below.

Adaptation of Theory for Stagnation-Point Probe

We have applied Lam's theory in developing a procedure for interpreting the current-voltage characteristics for a flat-faced cylindrical probe with an electrode at the stagnation point. The analysis is presented in detail in the Appendix. It is valid for incompressible flow, i.e., the ion and electron temperatures are taken to be constants, although not equal. Correction for compressibility effects is discussed later in this section.

For our probe geometry the resulting expressions for the positive ion and electron densities are:

$$J^{+}_{B,\mathrm{sat}} = en_{+\infty}\bar{I}[2Re_\infty(\bar{\beta}/LU_\infty)]^{1/2}D_i[1 + (T_e/T_i)]$$
$$J^{-}_{B,\mathrm{sat}} = en_{e\infty}\bar{I}[2Re_\infty(\bar{\beta}/LU_\infty)]^{1/2}D_e[1 + (T_i/T_e)] \quad (1)$$

The parameter $\bar{I}$ is plotted in Fig. 4.

Table 1 Representative flow parameters

	λ, 10^{-5} cm	y_{sh} (10v), 10^{-2} cm	δ, 10^{-3} cm	L, cm
Typical[a] sea-level rocket exhaust	0.6	0.7	8	0.42
Laboratory flame $n_e = n_+ = 10^{10}$ cm^{-3}	2.9	35.3	76	0.42
$n_e = n_+ = 10^{14}$ cm^{-3}	2.9	1.6	76	0.42

[a] Computed from conditions given in Table 3 of Ref. 2 for typical composite solid, propellant (9% Al) exhaust.

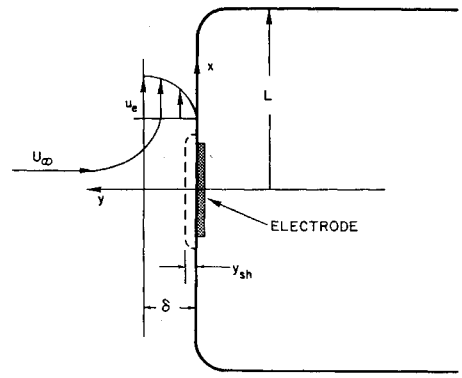

CHARACTERISTIC LENGTHS: λ, y_{sh}, δ and L

Fig. 3 Flowfield at probe tip.

The positive ion temperature can be assumed to be the same as that of the neutrals, because energy exchange between particles of nearly equal mass is efficient. The electron temperature is generally more uncertain. In the particular environments of present interest (atmospheric pressure laboratory flame and rocket exhaust), however, the assumption of electron temperature equilibration with neutral molecules was demonstrated to be reasonable. This is discussed more fully in the following section.

Special Considerations in Rocket Exhausts

When an electrostatic probe is used in a rocket exhaust, it is necessary to consider the following: 1) heat-transfer effects, 2) the possibility of shock-induced ionization, and 3) the presence of negatively charged ions.

To account for the heat-transfer effects (due to the cooled electrode), we used a recent analysis by Burke,[9] which is an extension of Lam's basic theory.[8] Burke's analysis assumes the ions are at the gas temperature, but evaluates the electron temperature by solving the electron energy equation. The solution of the resulting set of simultaneous differential equations (two diffusion, Poisson and the electron energy equations) is extremely difficult and costly in terms of computer time; however, in the two limiting cases of either frozen or equilibrium electron temperature, the problem is greatly simplified. By using an analysis similar to that of Chung and Mullen,[10] who studied electron temperature equilibration in a stagnation point boundary layer, we found that the electron temperature is nearly in equilibrium with the neutral

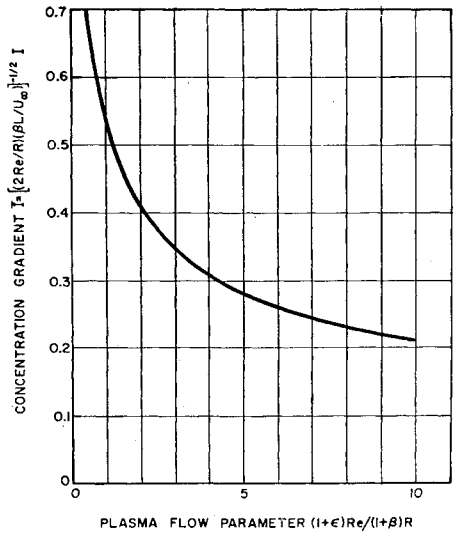

Fig. 4 Ambipolar concentration gradient at $\eta = 0$ for stagnation point of a flat-faced cylinder.

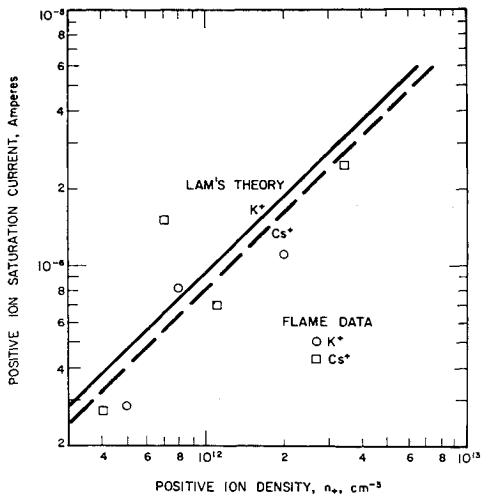

Fig. 5 Comparison of measured and calculated positive ion saturation currents.

gas temperature. This is due to the presence of large amounts of triatomic molecules (e.g., H_2O, CO_2) which can exchange energy very effectively with electrons.[11] Therefore we can consider the special case of Burke's equilibrium electron temperature compressible analysis. It was found in Ref. 9, that nonisothermal effects could be accounted for by a simple correction to the adiabatic analysis. The saturation currents for the cooled probe and uncooled stagnation-point probe were found to be in the simple ratio

$$\frac{J_{B,\text{sat,cooled}}}{J_{B,\text{sat,adiab}}} = \frac{\alpha'_1(0)_{\text{cooled}}}{\alpha'_1(0)_{\text{adiab}}} \left(\frac{T_\infty}{T_w}\right)^{0.5} \tag{2}$$

This expression holds for both positive and negative saturation currents. The $\alpha'_1(0)$'s in the above equation are proportional to the charged species concentration gradients. The actual values of $\alpha'_1(0)$ were obtained numerically by Burke for various wall temperature ratios (Fig. 1 in Ref. 9). For the case of electron temperature equilibrium, the values of $\alpha'_1(0)$ are insensitive to the current levels and can be tabulated as a function of the wall temperature ratio alone, as shown in Table 2.

A chemical kinetic analysis was performed to determine whether shock-layer ionization in supersonic portions of the rocket exhaust has to be considered. Taking into account the two major ion-production reactions,[12] i.e.,

$$K + M \rightleftarrows K^+ + e^- + M$$

$$K + Cl \rightleftarrows K^+ + Cl^-$$

we found that the ionization half-times were of the same order of magnitude as the residence time of the gas in the shock layer. Thus, shock-layer ionization may affect the probe measurements in the supersonic portions of the exhaust. However, for typical sea-level rocket exhausts, subsonic regions encompass a significant portion of the total plume.

The remaining theoretical consideration is the presence of negative ions in the plasma. Invoking charge neutrality, we take the sum of negative charges to be equal to the sum of positive charges. In the continuum saturation limit, the measured currents are proportional to the individual diffusion coefficients of the collected particles. Because the plasma is weakly ionized, the collection of electrons and negative ions is additive. Furthermore, $D_e \gg D_-$. Thus, the electron density in a plasma containing negative ions is given by the expression

$$n_e = n_+(D_-/D_e)[(J^-{}_{B,\text{sat}}D_+/J^+{}_{B,\text{sat}}D_-) - 1] \tag{3}$$

This method of calculation is limited to moderate ratios of negative ions to free electrons. When this ratio exceeds 10^3, the electron flux constitutes only a small fraction of the total negative current. Then the evaluation of n_e from Eq. (3) involves a small difference between two large quantities, and reliable values of n_e cannot be obtained. The indication that $n_e \ll n_+$ by use of the electrostatic probe could itself be a significant finding in estimation of radar interference effects.

Verification of Probe Theory

When this study began, Lam's theory had not been sufficiently verified experimentally. Partial verification of the theory in the limit of positive-ion saturation was reported by Brundin and Talbot,[7] and by Gordon.[13] Therefore, prior to application of Lam's theory in the rocket exhaust environment we decided to verify it in a laboratory flame where known levels of ionization can be produced by seeding with alkali metals. Although it is true that the laboratory flame does not fully simulate conditions in a rocket motor, it can duplicate many of the essential features of the theory. Sample conditions that can be produced in our laboratory flame are shown in Table 1. The ordering of length scales in the flames is the same as in a typical rocket exhaust.§ Thus, the same general theory should be applicable in both cases, and the laboratory flame can be used to test the validity of the general theory. The burner and flame system used are described in Ref. 14.

The results of our laboratory verification are presented in Fig. 5. For different levels of ionization in the flame (computed assuming thermochemical equilibrium to exist¶), Fig. 5 shows the measured saturation currents. Also shown are theoretically predicted saturation currents as a function of ionization level. The good agreement between theory and experiment provides additional verification of Lam's theory for positive ion collection. In these experiments it was not possible to obtain true electron saturation because the relatively large probe (compared to burner diameter) was collecting a large fraction of all the electrons present in the flame and thus was disturbing the plasma.

Electrostatic Probe Tests in Rocket Exhausts

Simulated Altitude Tests with Subscale Motors

A series of tests was conducted at the Naval Research Laboratory in a test chamber in which small rockets could be fired at subatmospheric pressure.[16] For most of the tests, the chamber pressure ranged from 80 to 200 torr (corresponding to altitudes of 16 and 10 km, respectively). The rocket motors had nozzle exit diameters of 0.3 to 0.5 in. and combustion times were typically on the order of 10 sec. The rocket motor grains were composite solid propellants containing up to 24% aluminum. The probe positions in the exhaust ranged from 10 to 31 in. from the nozzle exit plane and 0 to 6 in. from the motor axis. At these locations, the flow was subsonic and no shock formed in front of the probe. In the test facility, the motor could be either fixed in place or nutated** so that the probe would periodically be exposed to different portions of the exhaust.

The exhausts of highly aluminized propellants contain aluminum oxide particles, which adhere to the probe upon impact. After a brief period, the stagnation point electrode can be completely covered by a solid layer of aluminum oxide,

§ Note that for the low ionization levels in laboratory flames the requirement $y_{sh} \ll \delta$ is not completely satisfied.

¶ It has been shown experimentally[15] that an equilibrium calculation is valid under the conditions of these tests.

** Sketch in corner of Fig. 8 illustrates nutation in the present context.

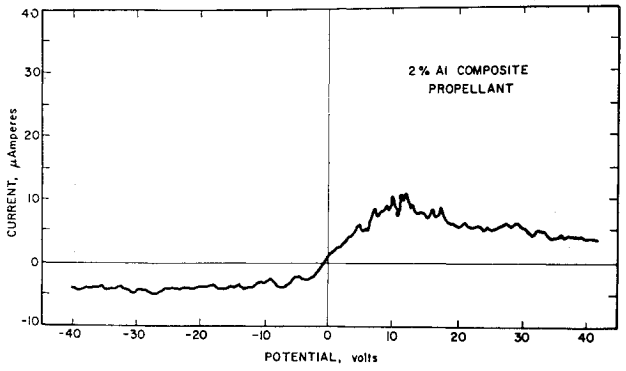

Fig. 6 Current-voltage characteristic (NRL test 3).

making it impossible to obtain any additional electrical measurements. To determine what occurs at different positions of the probe in the exhaust, a set of tests was made, with the probe position changed to expose the probe to progressively more severe conditions. As a result of these tests, we found that measurements could be made in highly aluminized exhausts, provided the probe was placed some distance†† off the axis of the motor (with the motor nutating, the off-axis distance is taken normal to the plane of nutation). The deposit of solid combustion products on the probe tip was large on the motor axis, becoming progressively less severe as the probe was moved toward the edge of the exhaust plume.

The remaining, and most important, objective of the NRL test program was to obtain electrostatic measurements in the rocket motor exhausts. Since many tests served simply to determine the mechanical integrity of the probe, and because in others the probe was deliberately placed in regions of the exhaust where coating was severe, interpretable data were obtained for only a limited number of runs. The current and voltage traces for two of these runs are shown in Figs. 6 and 7. Figure 6 shows that saturation was obtained at both positive and negative voltages. The slight decrease in the probe current after about +15 v is probably due to gradual buildup of solid combustion products on the probe tip. This trace was interpreted in terms of charged-species densities, using the theoretical analysis presented earlier in this paper.‡‡ In order to apply Eq. (1) it would be extremely useful to measure local values of temperature and velocity; however, without direct experimental information, we used the results of theoretical analyses. Furthermore, within the scope of the present study and for these preliminary tests, the accuracy of the temperature and velocity distributions was not critical. Consequently, these quantities were estimated via the velocity and temperature profiles given by Abramovich[18] and the measured jet spreading rates determined by Love.[19]§§ The resulting charged species

Table 2 $\alpha'_1(o)$ as a function of wall temperature ratio

T_w/T_∞	$\alpha'_1(0)$
1 (adiab.)	0.41
0.5	0.38
0.2	0.35
0.1	0.33

†† This off-axis position depends not only on propellant composition, but also on distance from the nozzle exit plane and on the nozzle exit diameter.

‡‡ The manner in which the diffusion coefficients were evaluated numerically is outlined in detail in Ref. 17.

§§ For the purpose of this study we could not utilize the more sophisticated techniques for analyzing afterburning solid propellant rocket exhausts.[20,21]

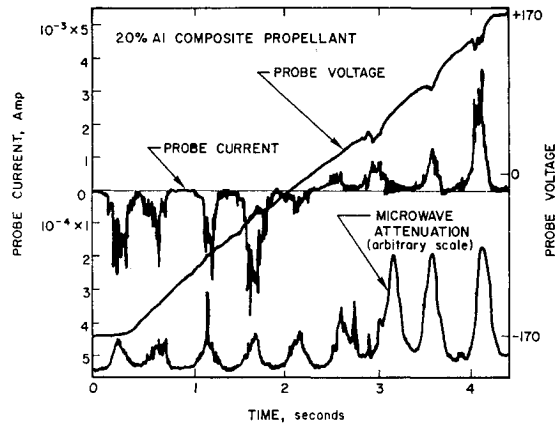

Fig. 7 Results of NRL test 315.

densities were $n_+ = 1 \times 10^{13}$ cm^{-3} and $n_e = 1 \times 10^{10}$ cm^{-3}.¶¶ In Fig. 7, it is also apparent that current saturation was obtained. (The periodic oscillations in the probe current are due to the nutation of the rocket motor.) The one high current peak that is observed at a probe voltage of +160 v probably is due to the growth of the sheath beyond the diffusion layer, in which regime saturation no longer exists. This behavior is frequently observed for all continuum probes at sufficiently high voltage. The data presented in Fig. 7 have been interpreted in terms of maximum charged species densities with the following results: $n_+ = 5 \times 10^{13}$ cm^{-3} and $n_e = 1 \times 10^{11}$ cm^{-3}.

A few tests were made with the motor nutating and the probe potential fixed at a voltage where saturation was expected. As the motor nutates, the probe is exposed to the rocket exhaust at various positions in the plume. The measured transient saturation currents can be interpreted in terms of a distribution of ion density across the plume. We analyzed the data for the plume traverse for one of these tests. The probe was located 0.9 in. from the plane of nutation and positive ions were collected with a probe potential at -60 v. The measured current for one of the traverses is shown in Fig. 8, plotted as a function of probe position in the exhaust (as illustrated in the sketch above the curves). The

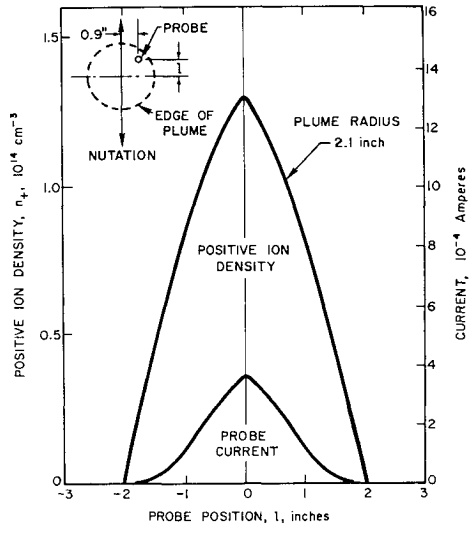

Fig. 8 Probe current and positive ion density across the plume (test 410).

¶¶ Note that the ratio of concentrations for negative ions and free electrons was 10^3; consequently the accuracy of n_e is open to question [see Eq. (3)]. This difference is most probably due to attachment of electrons to form Cl^-.

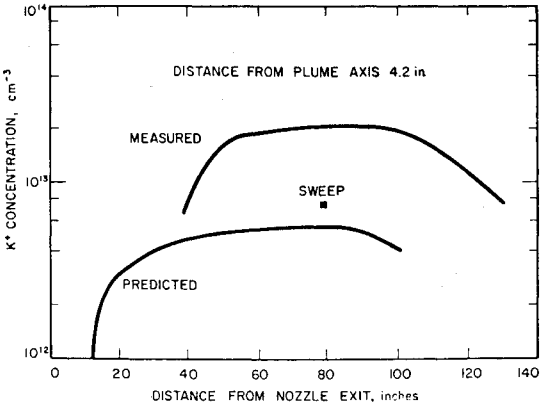

Fig. 9 Comparison between predicted and measured positive ion concentration.

peak current at the middle of the traverse was interpreted in terms of a positive ion density of 1.3×10^{14} cm^{-3}. The distribution of n_+ at other positions in the plume can be estimated by use of the proportionality relationship derived from Eq. (1),

$$n_+ \propto J^+_{B,\text{sat}} U^{-0.5} T^{-1.15} \tag{4}$$

The distribution of velocity and temperature across the exhaust plume at the probe position (18 in. from the exit plane) was estimated as described earlier. By using these estimated profiles and probe current distribution in Fig. 8, we obtained the positive ion density distribution across the plume; this also is plotted in Fig. 8. The ion density profile shows a sharp maximum at the axis of the plume.

Sea-Level Tests with Full-Scale Motors

A test program to measure local plasma properties at sea level for a 16% aluminum solid composite rocket propellant exhaust was conducted at Thiokol-Huntsville. The rocket motor used had a nozzle exit diameter of 3.75 in. The probe positions in the exhaust ranged from 20 to 120 in. from the nozzle exit and 1 to 4.2 in. from the motor axis. A typical sequence of events during these tests was the following: 1) the motor was ignited with the probe out of the plume, 2) after about 0.1 sec the probe was inserted into the plume, 3) with the radar cart (on which the probe was mounted) in a fixed position, the probe voltage was varied over a range of ± 45 v in 1 sec, and 4) with the probe kept at a fixed potential, the radar cart traversed the plume (total firing time was about 2.5 sec).

The experimental current-voltage traces were interpreted in terms of positive ion densities (for this solid propellant, the dominant positive ion is K^+). The results obtained with the probe at 4.2 in. from the plume axis are shown in Fig. 9. The single point labeled "sweep" was obtained from the positive ion saturation current, i.e., the probe was held fixed during this run, while a complete current-voltage sweep was obtained. The curve labeled "measured" was obtained from the local positive ion currents, while the probe was traversed along the length of the plume (attached to the radar cart). Also shown is the predicted K^+ concentration curve calculated via the techniques described in Ref. 20.*

Conclusions

It is concluded that electrostatic probe measurements of charged species concentrations in the severe thermal, abrasive and corrosive rocket exhaust environment can be obtained with properly designed electrostatic probes. While preliminary, these results demonstrated the potential value of the electrostatic probe as a diagnostic tool in measuring the microstructure of exhaust plumes.

* Ref. 20 shows that the predicted and measured radar attenuation (which is dependent upon the electron concentration) are in good agreement for this system. Thus, the predicted K^+ concentrations are reasonably accurate.

Appendix: Theoretical Analysis

In order to make use of Lam's theory it is necessary to reduce the generalized theory to a suitable form for interpreting data for the specific probe we have developed. This meant developing a procedure for interpreting the current-voltage characteristics for a flat-faced cylindrical probe with an electrode at the stagnation point. The analysis that follows relates to Lam's theory in its original form.

From Lam's generalized continuum theory, the expressions for the positive ion and electron saturation currents are given as

$$J^+_{B,\text{sat}} = en_{+\infty}(IR^{1/2}/L)D_i[1 + (T_e/T_i)] \tag{A1}$$

and

$$J^-_{B,\text{sat}} = en_{e\infty}(IR^{1/2}/L)D_e[1 + (T_i/T_e)] \tag{A2}$$

The parameter I, appearing in the above equations, is the charged-species concentration gradient at the edge of the sheath. It is computed from the ambipolar convection-diffusion equation as shown below. In Ref. 8, this equation is written in nondimensional form as (velocities are normalized by U_∞, x by L)

$$u(\partial N/\partial x) + vR^{1/2}(\partial N/\partial \eta) = [(1 + \epsilon)/(1 + \beta)] \times (\partial^2 N/\partial \eta^2) \tag{A3}$$

with the boundary conditions

$$\begin{aligned} \eta &\to \infty \quad N = 1 \\ \eta &\to \eta^*(x) > 0 \quad N = 0 \end{aligned} \tag{A4}$$

where η^* designates the outer edge of the sheath. Since the scale of the sheath is assumed to be much smaller than the scale of the ambipolar diffusion layer, a very small error is introduced by assuming $\eta^* \simeq 0$.

Writing Eq. (A3) in dimensional form (except for N), we have

$$u(\partial N/\partial x) + v(\partial N/\partial y) = (1 + \epsilon)/(1 + \beta) \times [(L/R)U_\infty](\partial^2 N/\partial y^2) \tag{A5}$$

and

$$\begin{aligned} y &\to \infty \quad N = 1 \\ y &\to 0 \quad N = 0 \end{aligned}$$

In order to obtain solutions to Eq. (A5), we must first reduce it to an ordinary differential equation. We used the Lees-Dorodnitsyn transformation[22] to accomplish this for our probe geometry [i.e., stagnation point flow around a flat-faced cylinder (Fig. 3)]. For our particular case, the transformation equations simplify to

$$\bar{s} = \rho\mu\bar{\beta}(x^4/4) \tag{A6}$$

and

$$\bar{\eta} = (2\rho\bar{\beta}/\mu)^{1/2} y \tag{A7}$$

Application of this transformation to Eq. (A5), along with the assumption that $(dN/d\bar{s})_e = 0$, leads to

$$(1 + \epsilon)/(1 + \beta)(Re/R)N'' + fN' = 0 \tag{A8}$$

where primes designate differentiation with respect to $\bar{\eta}$ and f is the velocity function in the boundary layer, i.e.,

$$f' = (u/u_e) \tag{A9}$$

For axisymmetric stagnation point flow, the variation of f

is described by

$$f''' + ff'' + \tfrac{1}{2}[1 - (f')^2] = 0 \qquad \text{(A10)}$$

with the boundary conditions

$$\bar{\eta} = 0 \qquad f = f' = 0$$
$$\bar{\eta} \to \infty \qquad f = 1 \qquad \text{(A11)}$$

This equation has been solved by Hartree[23] and we have utilized his tabulated results in solving Eq. (A8).

Since we do not require the full solution of Eq. (A8), but only $(\partial N/\partial \bar{\eta})_{\bar{\eta}=0}$, the latter can be obtained by direct integration. The resulting expression is

$$\bar{I} = \left(\frac{\partial N}{\partial \bar{\eta}}\right)_{\bar{\eta}=0} = \left\{\int_0^\infty \exp\left[-\int_0^{\bar{\eta}'} (f)\Big/\left(\frac{(1+\epsilon)Re}{(1+\beta)R}\right) d\bar{\eta}''\right] d\bar{\eta}'\right\}^{-1} \qquad \text{(A12)}$$

The integrals were evaluated numerically over the anticipated range of the parameter

$$[(1 + \epsilon)Re]/[(1 + \beta)R]$$

(i.e., from 0.5 to 10); the resulting curve is shown in Fig. 4. The concentration gradient $\bar{I}$ as plotted in Fig. 4 is in terms of the Lees-Dorodnitsyn coordinate $\bar{\eta}$. Since we require this gradient in Eqs. (A1) and (A2) in terms of Lam's coordinate $\eta = yR^{1/2}/L$, we must again make use of the transformation Eq. (A7). Thus,

$$\partial N/\partial \eta = [2(Re/R)(\bar{\beta}L/U_\infty)]^{1/2}(\partial N/\partial \bar{\eta}) \qquad \text{(A13)}$$

and

$$I = (\partial N/\partial \eta)_{\eta=0} = [2(Re/R)(\bar{\beta}L/U_\infty)]^{1/2}\bar{I} \qquad \text{(A14)}$$

Substituting the expression for I from Eq. (A14) into the equations for the positive ion and electron saturation currents, we obtain Eq. (1)

References

[1] Pergament, H. S. and Calcote, H. F., "Thermal and Chemi-Ionization Processes in Afterburning Rocket Exhausts," *Eleventh Symposium (International) on Combustion*, The Combustion Institute, Pittsburgh, 1967, pp. 597–611.

[2] Pergament, H. S. and Calcote, H. F., "A Mathematical Model for Predicting RF Interference Effects in Rocket Exhaust Plumes," *Proceedings of the Third Symposium on the Plasma Sheath—Plasma Electromagnetics of Hypersonic Flight*, Vol. II, Hanscom Field, Bedford, Mass., May 1967, pp. 309–354.

[3] Rice, W. E. et al, "Ionization Probes in Rocket Exhausts," Tech. Publ. 118, Nov. 1957, Experiment Inc., Richmond, Va.

[4] Mott-Smith, H. M. and Langmuir, J., "The Theory of Collectors in Gaseous Discharges," *Physical Review*, Vol. 28, 1926, pp. 727–763.

[5] Su, C. H. and Lam, S. H., "Continuum Theory of Spherical Electrostatic Probes," *The Physics of Fluids*, Vol. 6, No. 10, Oct. 1963, pp. 1479–1491.

[6] Cohen, I. M., "Asymptotic Theory of Spherical Electrostatic Probes in a Slightly Ionized, Collision-Dominated Gas," *The Physics of Fluids*, Vol. 6, No. 10, Oct. 1963, pp. 1492–1499.

[7] Talbot, L., "Theory of the Stagnation-Point Langmuir Probe," *The Physics of Fluids*, Vol. 3, 1960, pp. 289–298.

[8] Lam, S. H., "A General Theory for the Flow of Weakly Ionized Gases," *AIAA Journal*, Vol. 2, No. 2, Feb. 1964, pp. 256–262.

[9] Burke, A. F., "Theoretical Studies of Continuum, Weakly Ionized Gas Flows Including Compressibility and Electron Energy Effects," May 1967, PhD dissertation, Princeton Univ., Princeton, N.J.; also AN-2101-Y-1, Cornell Aeronautical Lab., Buffalo, N.Y.

[10] Chung, P. M. and Mullen, J. F., "Nonequilibrium Electron Temperature Effects in Weakly Ionized Stagnation Boundary Layers," Rept. TDR-169 (3230-12) TN-7, May 20, 1963, Aerospace Corp., San Bernardino, Calif.

[11] Cottrell, T. L. and Walker, I. C., "Drift Velocities of Slow Electrons in Polyatomic Gases," *Transactions of the Faraday Society*, Vol. 61, 1965, pp. 1585–1593.

[12] Jensen, D. E., "Chemical Kinetics in Rocket Exhaust Plasmas," TP-204, April 1969, AeroChem Research Labs., Princeton, N.J.

[13] Gordon, S. A., "The Use of Ionization Probes to Determine Rocket Motor Parameters," Final Rept. AFRPL-TR-65-208, DDC AD 474 517; TP-120, Nov. 1965, AeroChem Research Labs., Princeton, N.J.

[14] Jensen, D. E., "Production of Electrons from Alkaline Earths in Flames: Equilibrium and Kinetic Considerations," *Combustion and Flame*, Vol. 12, 1968, pp. 261–268.

[15] Jensen, D. E. and Padley, P. J., "Dissociation Energies of the Alkali Metal Hydroxides," *Transactions of the Faraday Society*, Vol. 62, 1966, pp. 2132–2139.

[16] Balwanz, W. W., "Ionization in Rocket Exhausts," *Tenth Symposium (International) on Combustion*, The Combustion Institute, Pittsburgh, Pa., 1965, pp. 685–697.

[17] Maise, G. and Sabadell, A. J., "Determination of the Electrical Characteristics of Rocket Exhaust Plumes with Electrostatic Probes," Final Rept. AFRPL-TR-68-135, DDC AD 843 505; TP-172, April 1968, AeroChem Research Labs., Princeton, N.J.

[18] Abramovich, G. N., *The Theory of Turbulent Jets*, M.I.T. Press, Cambridge, Mass., 1963, p. 19.

[19] Love, E. S. et al., "Experimental and Theoretical Studies of Axisymmetric Free Jets," TR-R-6, 1959, NASA.

[20] Pergament, H. S., "The Role of Eddy Viscosity Models in Predicting Afterburning Rocket Exhaust Plume Properties and Radar Attenuation," TP-199, April 1969, AeroChem Research Labs., Princeton, N.J.

[21] Smoot, L. D. and Purcell, W. E., "Model for Mixing of a Compressible Free Jet with a Moving Environment," *AIAA Journal*, Vol. 5, No. 11, Nov. 1967, pp. 2049–2052.

[22] Lees, L., "Laminar Heat Transfer Over Blunt-Nosed Bodies at Hypersonic Flight Speeds," *Jet Propulsion*, Vol. 26, 1956, pp. 259–269 and 274.

[23] Hartree, D. R., "On An Equation Occurring in Falkner and Skan's Approximate Treatment of the Equations of the Boundary-Layer," *Proceedings of the Cambridge Philosophical Society*, Vol. 33, 1927, pp. 223–239.